Environmental Science and Pollution Research (2019) 26:10363–10373
https://doi.org/10.1007/s11356-019-04375-z

RESEARCH ARTICLE

Effect of irrigation amount and fertilization on agriculture non-point source pollution in the paddy field

Huiliang Wang[1] · Peng He[1] · Chenyang Shen[1] · Zening Wu[1]

Received: 1 October 2018 / Accepted: 24 January 2019 / Published online: 14 February 2019

Abstract

It is the key point to reveal the effect of irrigation water and fertilization conditions on the agriculture non-point pollution in the paddy field. In this study, the estimation model of agricultural non-point source pollution loads at field scale was established on the basis of agricultural drainage irrigation model and combined with pollutant concentration predication model. Based on the estimation model of agricultural non-point source pollution in the field and experimental data, the load of agricultural non-point source pollution in different irrigate amount and fertilization schedule in paddy field was calculated. The results showed that the variation of field drainage varies greatly under different irrigation conditions, and there is an "inflection point" between the irrigation water amount and field drainage amount. The non-point pollution load increased with the increase of irrigation water and showed a significant power correlation. Under the different irrigation condition, the increase amplitude of non-point pollution load with the increase of irrigation water was different. When the irrigation water is smaller, the non-point pollution load increase relatively less, and when the irrigation water increased to inflection point, the non-point pollution load will increase considerably. In addition, there was a positive correlation between the fertilization and non-point pollution load. The non-point pollution load had obvious difference in different fertilization schedule even with same fertilization level, in which the fertilizer pollution load increased the most in the period of turning green to tillering. The results provide some basis for the field control and management of agricultural non-point source pollution.

Keywords Agricultural non-point source pollution · Pollution load intensity · Irrigation · Fertilizers · Fertilization schedule

Introduction

Over the last few decades, water quality has become a challenging issue, threatening the security of society and ecosystems in China. Agricultural non-point source pollution, which was caused by chemical fertilizer and pesticide especially, contributes in a major way to the declining water quality of aquatic systems, such as lakes and rivers, in most cases (Bryan 2011; Lu and Xie 2018). In agricultural production activities, with the dynamic action of irrigation water (precipitation), various pollutants (nutrients, pesticides, bacteria, etc.) spread from soil circle to water circle in the form of low concentration and large range through farmland surface runoff, farmland drainage, and underground leakage, and the pollutants may cause eutrophication and thus impact aquatic ecology. Accordingly, water pollution control programs are often established to control agricultural non-point source pollution (Ongley et al. 2010; Li et al. 2018). Studies confirmed that non-point sources of these pollutants contributed much more than point sources in agricultural areas. For example, Azzellino et al. (2006) found that the non-point sources contributed to around 80% in the areas with extensive agricultural activities. A study in the Taihu Lake catchment showed that total N and total P from non-point sources contributed to 92% and 75% of the whole input, respectively (Li et al. 2010), and similar results were observed in studies of other catchments (Du et al. 2014). Because of this wide range, the difficulty of control agricultural non-point source pollution and complex uncertainties, agricultural non-point source pollution has also become a focus in the field of water pollution control worldwide (Shen et al. 2013). How to quantify the agricultural non-point source pollution loads reliably is the key to implement watershed management practices.

Responsible editor: Philippe Garrigues

✉ Zening Wu
zeningwu@zzu.edu.cn

[1] College of Water Conservancy & Environmental Engineering, Zhengzhou University, Zhengzhou 450001, Henan, People's Republic of China

Methods for estimating the load of agricultural non-point source pollution include modeling in watershed scale (Wu et al. 2015; Moges et al. 2018) and small-scale field experiment (Pratt 2012; Chen and Lu 2014). The modeling method is preferred by many researchers, but those models typically require various types of data such as soil properties, vegetation of catch basin, and rainfall data (Arnold et al. 1998; Bicknell et al. 2011). The ability of numerical models is limited by data limitation or data sparse, such as incomplete understanding of the processes involved and inaccuracies in model formulation (Li et al. 2010; Wang et al. 2015a), invalid values of model parameters (Shen et al. 2008; Wang et al. 2015b), and inadequate or erroneous information needed to apply the models such as input and calibration data (Price et al. 2014; Wang et al. 2015c). Moreover, the models focus on non-point source pollution induced by water and soil erosion; in other words, in the watershed non-point source pollution, the whole process and characteristics of agricultural non-point source pollution were less considered (Li et al. 2018). In fact, according to the characteristics of agricultural non-point source pollution, the whole process of agricultural non-point source pollution can be divided into the "source" link of field pollution production and the "sink" link of water transportation through drainage channels (Wriedt and Rode 2006; Haas et al. 2017). The source link is the key link of agricultural non-point source pollution control and management. Water flushing and leaching induced by irrigation or precipitation is the main inducement, which leads the agricultural non-point source pollutants to separate out from the fields. So, water is a necessary and sufficient condition for non-point source pollution; meanwhile, agricultural non-point source pollution was aggravated by field fertilization and accumulated nutrients among the field (Woodward et al. 2013). Field water and fertilization process are two main factors that determine the intensity of field production of agricultural non-point source pollution. The underlying question is how to establish a field-scale agricultural non-point source pollution load estimation model and quantitative the effect of water and fertilization process on agricultural non-point source pollution.

The objective of this study is to quantitative the effect of irrigation amount, fertilizer application amount, and fertilization scheme on agricultural non-point source pollution by combining the field experiment observation and field-scale agricultural non-point source pollution load estimation model. First on the basis of agricultural non-point source pollution monitoring and field experiment, the agricultural non-point source pollution model is proposed based on pulse incident. Then, the agricultural non-point pollution load is calculated in different irrigation water, fertilizer process, and fertilizer on cultivator. Finally, the relationship between agricultural non-point pollution and water and fertilization process is quantified.

Methods and materials

Model established

The process of agricultural non-point pollution load induced by irrigation and fertilization is mainly affected by two factors, one is the amount of farmland irrigation and the other is pollutant concentration in agricultural wastewater from drainage. The load process available is expressed as Eq. (1).

$$Wp(t) = \int_{t1}^{t2} Q(t)c(t)dt \quad (1)$$

where $W_p(t)$ is the agricultural non-point pollutant loading for farmland drainage process (mg d^{-1}), $Q(t)$ is the water discharge of the farmland drainage process (L d^{-1}), $c(t)$ is the pollutant concentration process in farmland drainage (mg d^{-1}), and t_1 and t_2 are the estimated starting and ending dates.

In Eq. 1, $Q(t)$ is calculated by DRAINMOD. The DRAINMOD model utilizes the principle of the balance between the overland water and the internal water flow of the soil to predict the change process of the water table, the overland and underground displacement, and the soil moisture content. In the calculation process of the model, the soil is automatically divided into saturated and unsaturated zones, and the unsaturated zone is considered as a one-dimensional vertical soil water movement, ignoring the influence of lateral soil water movement, while the saturated zone takes vertical and lateral soil water movement into account, and then calculates the balance of surface and underground soil water, respectively. More about DRAINMOD can be found in reference by Skaggs et al. (2012) descripted. $c(t)$ is calculated based on the transfer function model, which characterizes the output of the solute as a function of input flux, and the kinetic process of solute in the soil can be represented by a probability density function (White et al. 1986; Rinaldo et al. 2015), using the Eq. (2) calculation.

$$c_{\text{out}}(t) = \int_0^{\infty} c_{\text{in}}\left(t-t'\right) f\left(t'\right) dt' \quad (2)$$

In Eq. (2), $C_{\text{in}}(t-t')$ is the agricultural non-point pollutant concentration injected into the soil at the time t' before the simulation time t (mg/L), which is equivalent to the "synthesis" of fertilization and subsequent irrigation process by each farmland. In addition, the impact of fertilizer intensity and amount of irrigation can be reflected. $C_{\text{out}}(t)$ is the mass concentration of agricultural non-point pollutants in farmland drainage when $C_{\text{in}}(t-t')$ pulse concentration is injected into the soil (mg/L). $f(t)$ is a comprehensive function, which the essence is to inject pollutant concentration of unit hydrograph of pulse input into the field when the concentration of pollutants contained in the field drainage is selected, and the

inverse Gaussian distribution, as shown in Eq. (3), is used to calculated $f(t)$.

$$f(t) = \sqrt{\frac{\lambda}{2\pi t^3}} \exp\left[\frac{-\lambda(t-\mu)^2}{2\mu^2 t}\right] \tag{3}$$

In Eq. (3), λ and μ are two important statistical parameters in the inverse Gaussian distribution, which determine the shape of the curve, that is, the pollutant concentration of unit hydrograph. The range of values of λ and μ are both $(0,\infty)$. The initial value of λ and μ can be, respectively, calculated by the moment method and the maximum likelihood estimation method, which are shown in Eqs. (4) and (5).

$$\mu = \sum_{i=1}^{n} xi \tag{4}$$

$$\lambda = \frac{\bar{x} \bullet \mu^2}{\frac{1}{n}\sum_{i=1}^{n}\left(x_i - \bar{x}\right)^2} \tag{5}$$

where n is the number of monitoring and x_i is the monitoring data of the ith. The initial value can be determined by monitoring test data and further preferred.

The model was evaluated using the observed data of the drain outlet. The objective function used in model calibration was coefficient of determination (R^2), Nash-Sutcliffe coefficient (*NSE*), and relative error (*RE*), which are defined as follows (Du et al. 2019):

$$R^2 = \left(\frac{\sum_{i=1}^{n}\left(y_{sim}^i - \bar{y}_{sim}\right)\cdot\left(y_{obs}^i - \bar{y}_{obs}\right)}{\sqrt{\sum_{i=1}^{n}\left(y_{sim}^i - \bar{y}_{sim}\right)^2 \cdot \sum_{i=1}^{n}\left(y_{obs}^i - \bar{y}_{obs}\right)^2}}\right)^2 \tag{6}$$

$$NSE = 1 - \frac{\sum_{i=1}^{n}\left(y_{sim}^i - y_{obs}^i\right)^2}{\sum_{i=1}^{n}\left(y_{sim}^i - \bar{y}_{obs}\right)^2} \tag{7}$$

$$RE = \frac{\sum_{i=1}^{n}\left(y_{sim}^i - y_{obs}^i\right)}{\sum_{i=1}^{n} y_{obs}^i} \times 100\% \tag{8}$$

where y_{sim}^i is the simulated pollutant load in the i moment, y_{obs}^i is the observed pollutant load in the i moment, $\bar{y}_{obs}$ is the average observed pollutant load of simulated period, and $\bar{y}_{sim}$ is the average simulated pollutant load of simulated period.

Experimental layout and water sample monitoring

The project experimental area is located in Ding Village, Wangcun Town, Xingyang City, Zhengzhou City, where rice is grown. The length of the test area is about 1000 m; the field drainage is mainly open channel; the agricultural ditch is arranged in parallel at equal intervals; the spacing is l00 m; the ditch depth is 80–100 cm, showing a "*u*"-shaped section; the upper mouth is l00 cm; and the agricultural ditch controls farmland drainage. The area is about 0.1km^2 and the test was carried out from June to October 2017. Two drainage channels were designed. Among them, the drainage ditch 1 is used for model rate determination, while the model parameters are acquired, and the drainage ditch 2 is used for model verification. The application of parameters and model were determined to study the quantitative relationship between agricultural water and non-point source pollution under different water and fertilization conditions.

The test field's sowing is completed in early May, and the irrigation is started on June 10. The field irrigation and water withdrawal are monitored by the canal head and the measuring trough at the end of the agricultural ditch. Starting from June 11, the farmland withdrawal begin at the end of the agricultural ditch, while water samples are taken once every 6 days until the end of the water withdrawal. The water withdrawal process monitoring uses flow measurement weir.

In addition to the application of basic fertilization before planting, urea is applied in different growth stages in the experimental field. The specific fertilization process is shown in Table 1.

The water sample is extracted at a water depth of 1/2 by the middle twist line method and collected 1000 mL each time. According to the "Water and Wastewater Monitoring and Analysis Method" (4th edition), the COD is measured by potassium dichromate, while the ammonia nitrogen analyzed by ion chromatographically.

Data sources

The meteorological data such as the daily maximum and minimum temperature and the daily precipitation required by the DRAINMOD model are based on the data of the Xingyang Meteorological Bureau in the test area. The soil side guide water rate is measured by the drilling method on site, and soil moisture characteristic curve is determined by laboratory using centrifuge method, and other parameters can be converted according to the model principle.

Results

Model validation

COD and ammonia nitrogen load estimation in study field was calculated by the model established in above. In different growth periods of rice and in combination with different fertilization processes, the initial values were calculated

Table 1 Fertilization of experimental field process statistics

Different growth stages of rice	Data of fertilization	Type of fertilization	Amount of fertilization (kg/hm^2)	Net content of nutrient (kg/hm^2)
Base fertilizer	Before planting	Ammonium bicarbonate	800	141.6
Top dressing in turning green-tillering	July 8	Urea	300	135
Top dressing in jointing-heading	August 6	Urea	375	168.75

separately, and further fitting optimization was carried out by combining the measured data. The results are shown in Table 2.

Model's potential to predict observed COD and ammonia nitrogen load data is firstly assessed. Results of COD and ammonia nitrogen load calibration for the first agricultural drain are shown in Fig. 1.The simulated COD and ammonia nitrogen load followed the pattern similar to the observed values. *NSE*, R^2, and *RE* of the COD load between simulated and observed were calculated to be 0.83, 0.85, and − 11.2%, and *NSE*, R^2, and *RE* of the ammonia nitrogen load between simulated and observed were calculated to be 0.76, 0.88, and − 14.3%, respectively, implying that simulated COD and ammonia nitrogen load fit observed ones reasonably well. The second agricultural drain is used for model validation, shown in Fig. 2b. *NSE*, R^2, and *RE* of the COD load during validation drain are calculated to be 0.79, 0.82, and 10.4%, respectively, and *NSE*, R^2, and *RE* of the ammonia nitrogen load during validation drain are calculated to be 0.75, 0.81, and 9.7%, respectively.

Relationship between irrigation amount and drainage water volume

In order to quantitatively analyze the relationship between different irrigation and drainage water volume in the experimental field, combined with the previous irrigation system in the study area, this study designed the different amount of irrigation, which is measured at the weir of the irrigated canal intake descripted by field depth, from 22 to 68 cm, and applied that to the model established in the previous section under the specific 2017 atmosphere conditions, calculated the corresponding agricultural land drainage volume under different irrigation water conditions from June to October in the crop growth period. The results were shown in Table 3.

It can be seen from the data in Table 3 that with the increase of irrigation amount, the drainage water volume also shows an increasing trend, but with the increase of irrigation amount, the extent of the increase in drainage water volume is different. Further analysis was shown in Fig. 3.

In Fig. 3, the power correlation is tested by significance, which indicates that there is a significant correlation between the drainage water volume and the irrigation amount. It can be seen from Fig. 3 that under the different irrigation conditions, the variation range of drainage water volume is quite different. Combined with the relevant data in Table 3, When the irrigation water increased from 22 to 42 cm, the irrigation water increased by 20 cm while the drainage water volume increased by 11.92 cm, about 66.22% of the added value of irrigation water. Then the irrigation water increased from 42 to 68, irrigation water increased 26 cm, and the drainage water volume increased by 22.48 cm, accounting for 86.46% of irrigation water. So there is an "inflection point" between the irrigation water amount and drainage water volume. When the amount of irrigation is below the inflection point, the relative increase in drainage water volume is small, and when the amount of irrigation is greater than the value of inflection point, the increase in drainage water volume is large. It can be seen from the shape of the power curve in Fig. 3 that the inflection point between the irrigation and drainage water volume relationships in the study area is about 42 cm of irrigation amount.

Table 2 Initial parameters and optimum results of λ and μ

Different growth stages of rice	COD				Ammonia nitrogen			
	Initial parameters		Optimum parameters		Initial parameters		Optimum parameters	
	λ	μ	λ	μ	λ	μ	λ	μ
Seedling	20	300	22	393	25	200	37	216
Turning green-tillering	20	300	24	521	25	200	44	346
Jointing-heading	20	300	19	424	25	200	44	325

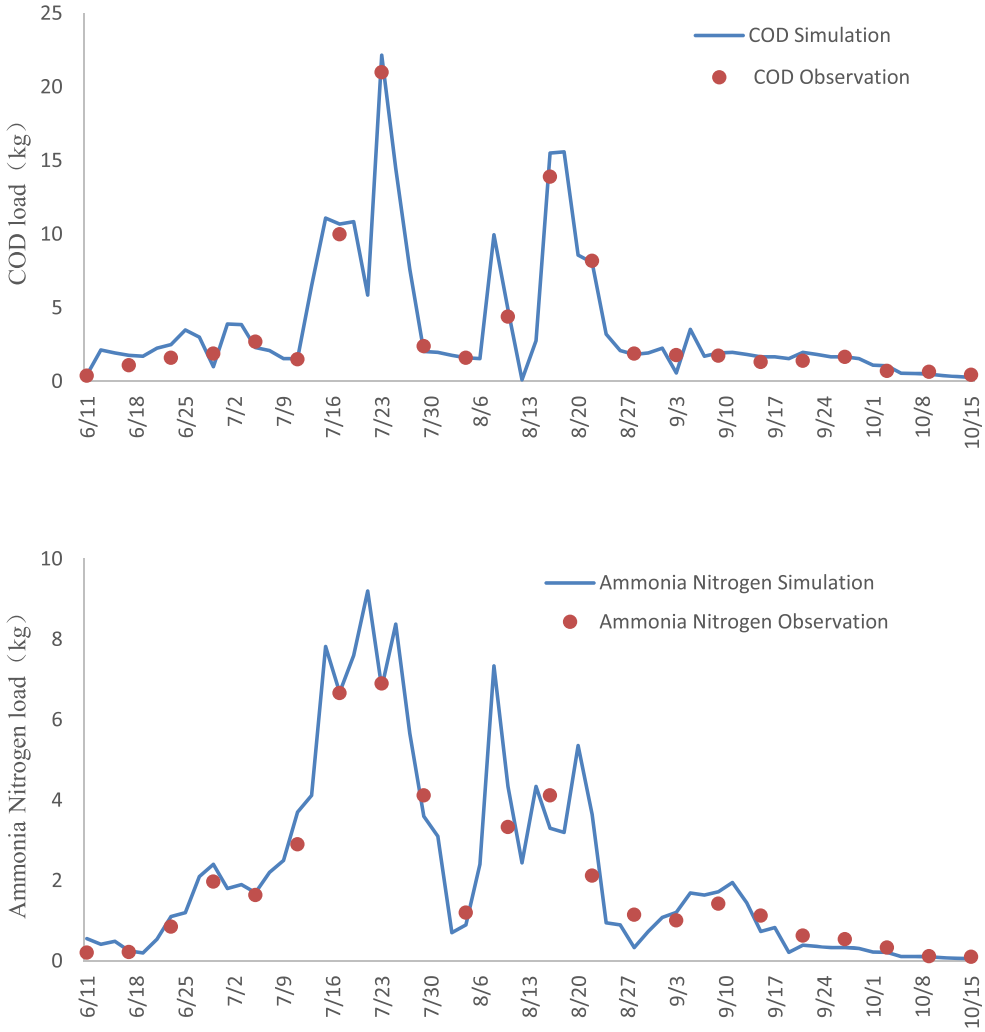

Fig. 1 Calibration for loading of COD and ammonia nitrogen in the first agricultural drain

Relationship between irrigation amount and total pollution load

It can be seen from the previous model formulas (1) and (2) that under certain conditions, the influence of irrigation amount on the field pollution load is mainly reflected in two aspects. First, the increase of irrigation amount leads to an increase in field drainage, then the concentration is equivalent to increasing the pollution load in the field; the second is that the increase of irrigation amount can reduce the concentration of "fertilization solution" injected into the soil, which is equivalent to reduce the field pollution load. In addition, the increasing of field irrigation increases the washing and leaching intensity of agricultural non-point source pollutants in the soil, and promoted the non-point source pollutants.

On the basis of the above analysis of the relationship between field irrigation and drainage, based on the monitoring data of field fertilization in the test area in 2017, the previous model is used to calculate the field pollution load under different irrigation conditions between 22 and 68 cm. The results were shown in Table 4.

In order to further analyze the relationship between the irrigation amount and the field pollution load, the correlation analysis between the field irrigation amount and the pollution load in Table 3 is made, as shown in Fig. 4.

The correlation in Fig. 4 shows that there is a significant positive correlation between the field pollution load and the irrigation amount through the significance test. It can be seen from the calculation results in Table 4 and Fig. 4 that the relationship between the amount of irrigation and the pollution load is similar to the relationship between the irrigation amount and the drainage water volume and that two characteristics still show: (1) the field pollution load increases with the increase in irrigation amount and (2) the field pollution load increases with the increase in irrigation amount under different irrigation conditions. When the irrigation amount is small, the field pollution load increases rapid relatively. But when the irrigation amount increases to about 42 cm, the field pollution load increases more. It is noted that 42 cm is an inflection point between the irrigation water amount and drainage water volume in this study, which is not all over studies. But, the method to find this inflection point is a universal method.

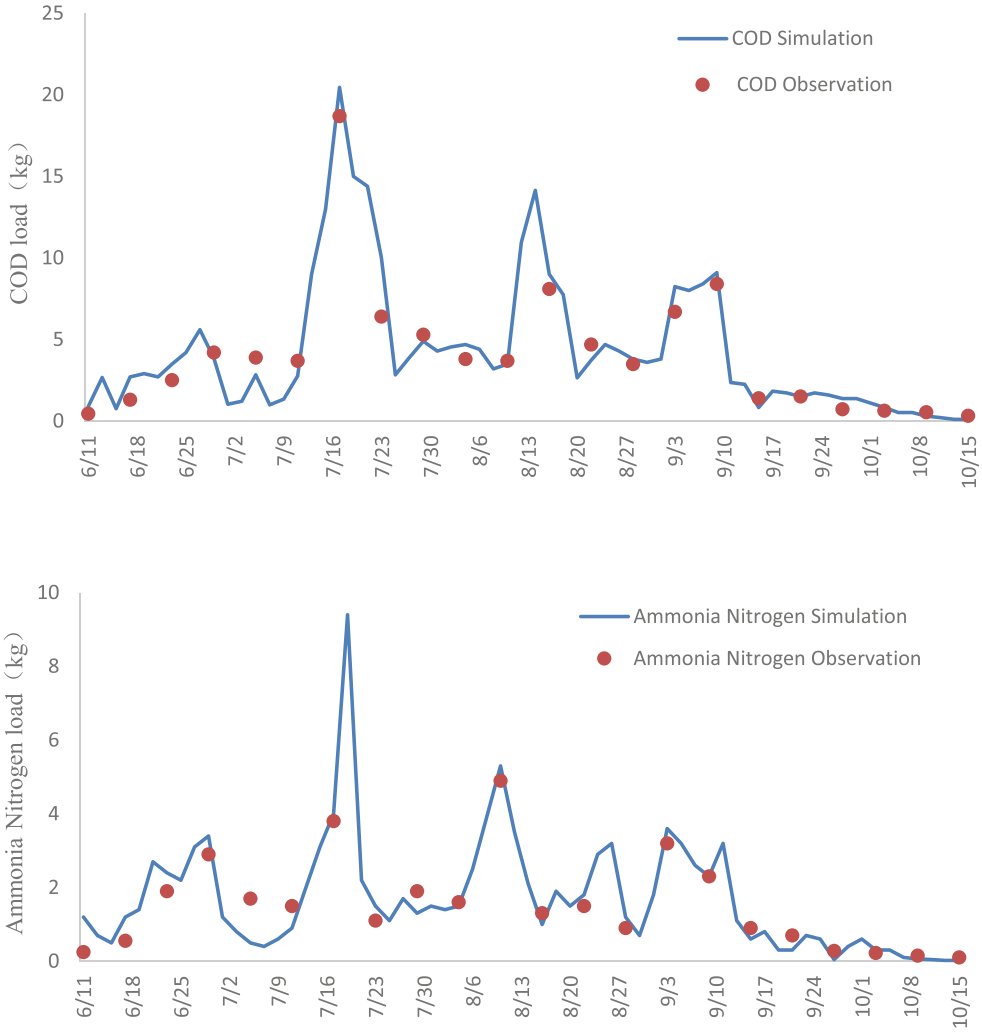

Fig. 2 Validation for loading of COD and ammonia nitrogen in the second agricultural drain

Relationship between fertilizer application and total pollution load

Field fertilization is the main source of non-point source pollutant in agriculture. The amount of fertilizer applied has a great influence on the field pollution intensity. Under the assumption that the other external conditions such as the actual irrigation water amount are unchanged in the test area in 2017, taken the current experimental application of the 2017 experimental field as the basic plan, and the application amount of the base fertilization, the July topdressing and the August topdressing are adjusted, respectively, and a total of 15 different designs are designed. The fertilization schemes were shown in Table 5. Among them, Scheme 1 to Scheme 5 changes in the amount of basic fertilization, and the topdressing is unchanged; Scheme 6 to Scheme 10 is the change of topdressing amount in turning green-tillering and the basic fertilization and topdressing amount in jointing-heading are unchanged, and Scheme 11 to Scheme 15 is the change of topdressing amount in jointing-heading and basic fertilization and the amount of topdressing remained unchanged in turning green-tillering. The field pollution load under different fertilization schemes is calculated by using the preceding model, and the results were shown in Table 4.

It can be seen that under different fertilization schemes, the field pollution load increases linearly with the increasing of

Table 3 Relationship between irrigation amount and drainage water volume

Irrigation amount (cm)	Drainage water volume (cm)	Ratio of drainage to irrigation
22	5.72	0.26
27	7.83	0.29
34	11.9	0.35
42	17.64	0.42
50	25.5	0.51
59	31.27	0.53
68	40.12	0.59

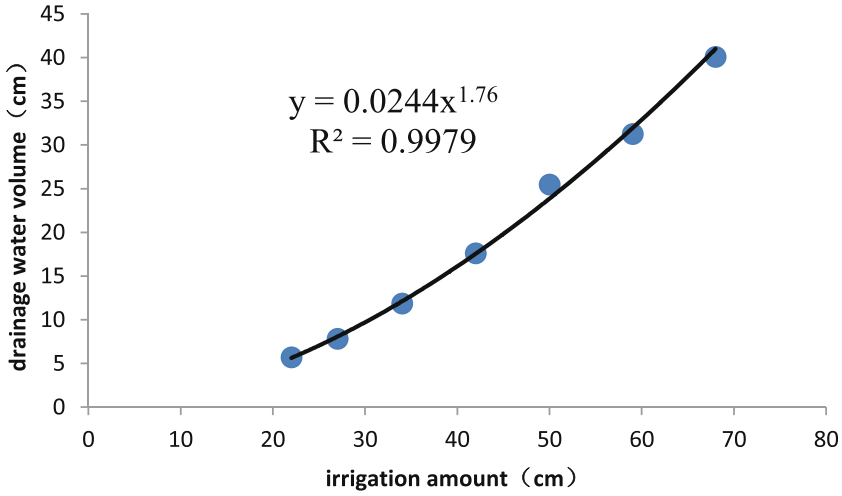

Fig. 3 Relationship between irrigation amount and drainage water volume

fertilization application. On the one hand, the increasing of the amount of fertilization in the field increases the concentration of pollutants entering the surface runoff of the farmland. On the other hand, under the hydrodynamic action, the pollutants move vertically downward, which also increases the pollution in the field drainage and may causes deep groundwater pollution. Table 4 also shows that under different fertilization schemes, the field pollution load increases differently with the amount of fertilizer applied. Under the scenario of 40 kg/hm^2 of basic fertilization amount, first topdressing amount and second topdressing amount, the field pollution load of COD increases, respectively, by 11.25%, 16.13%, and 22.25%, while the ammonia nitrogen of the field pollution load increased by 8.33%, 22.09%, and 48.72%.Therefore, whether it is the field pollution load of COD or ammonia nitrogen, the second topdressing has the greatest impact, then the first topdressing followed, and finally the basic fertilization amount has the least impact. That is to say, in the case of increasing the amount of unit fertilization application, the pollution load of the second topdressing field unit increases the most, while the strength of the basic fertilization applied increases the least. It shows that even if the fertilization amount is the same and the fertilization scheme is different, the field pollution load will be greatly changed. And then, from the rate of change of the field pollution load of COD and ammonia nitrogen, the fertilization scheme has a greater impact on the pollution load of ammonia production.

Table 4 Relationship between field irrigation amount and pollution load

Irrigate amount (cm)	COD load (kg)	Ammonia nitrogen load (kg)
22	30.77	9.60
27	33.37	10.93
34	35.63	11.27
42	38.93	12.00
50	40.70	12.40
59	41.77	13.37
68	42.83	13.70

Discussion

According to the specific situation of the study area, fertilization in paddy field mainly includes basic fertilization and top dressing. Basic fertilization are generally applied before sowing, creating good soil conditions, improve soil and fertility for the growth and development of crops, and the depth of basic fertilization application is usually topsoil. Top dressing is generally applied during the growth of crops, and its function is mainly to supply a large amount of nutrients in a certain period of time, or to supply the basic fertilization deficiency. Paddy field top dressing generally adopts applicator way; the nutrients needed for the growth, such as nitrogen and phosphorus, can enter the activity layer of crop root under hydrodynamic action. In different fertilization schemes, the field pollution load is also different.

Based on the basic scheme in Table 5, this paper analyzes the sensitivity of the change of fertilization application under different fertilization schemes to the field pollution load and the change rate of COD load in field, as shown in Fig. 5.

As shown in Fig. 5, the second top dressing process in jointing-heading is the most sensitive to the increase of the field pollution load of COD in three different fertilization schemes, followed by the first top dressing process in turning green-tillering. In comparison, the change of the amount of basic fertilization has little effect on the pollution load of COD. Combined with the relevant data in Table 4, in comparison between the Scheme 1 and Scheme 2, the total amount of fertilization increased by 10 kg/hm^2, and the field pollution load of COD increased by 0.27 kg/hm^2.In comparison with Scheme 6 and Scheme 7, the total fertilization also increased by 10 kg/hm^2, and the field pollution load of COD increased

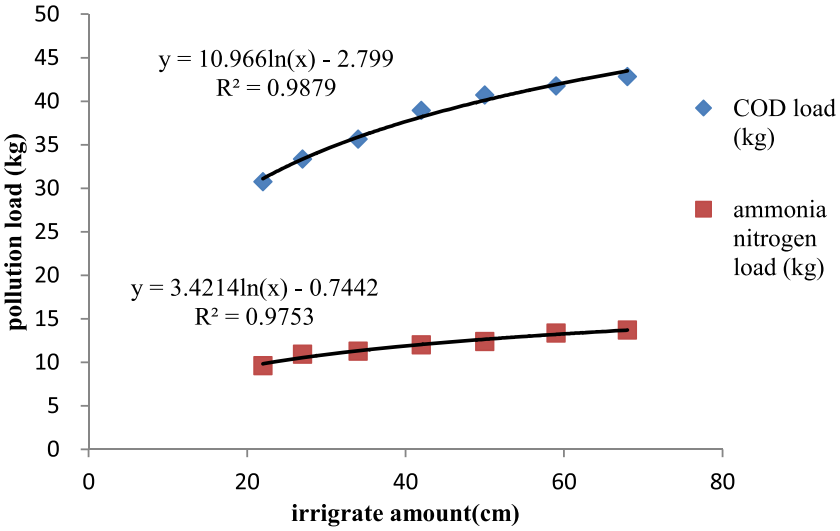

Fig. 4 Relationship between irrigation amount and field pollution load

by 0.43 kg/hm^2. In comparison with Scheme 11 and Scheme 8, the total fertilization also increased by 10 kg/hm^2, and the field pollution load of COD increased by 0.54 kg/hm^2. It can be seen that even with the same amount of fertilization and different fertilization schemes, there are significant differences in the variation of field pollution load of COD. For comparison among different fertilization schemes, such as Scheme 3 and Scheme 8, the total amount of nutrient applied in Scheme 3 is 443.75 kg/hm^2, and the COD load of field pollution is 11.42 kg/hm^2. The total amount of nutrient applied in Scheme 8 is 440.35 kg/hm^2, and the COD load of field pollution is 11.67 kg/hm^2. The total amount of nutrient applied to Scheme 8 is greater than that of Scheme 3, but the field pollution load of COD is less than Scheme 3.

The field pollution load of ammonia nitrogen is affected by different fertilization schemes as shown in Fig. 6.

It can be seen from Fig. 6, in other cases, only the change of the amount of basic fertilization, the amount of first top dressing and second top dressing, the slope of the relationship between the rate of change of fertilization application and the

Table 5 Different fertilization schemes and statistics on pollution load

Fertilization schemes		Net content of nutrient in base fertilizer (kg/hm^2)	Net content of nutrient in top dressing in turning green-tillering (kg/hm^2)	Net content of nutrient in top dressing in jointing-heading (kg/hm^2)	Net content of nutrient (kg/hm^2)	COD load (kg)	Ammonia nitrogen load (kg)
Basic schemes		141.6	135	168.75	445.35	39.53	12.77
Change base fertilizer	Scheme 1	120	135	168.75	423.75	36.13	12.40
	Scheme 2	130	135	168.75	433.75	37.03	12.53
	Scheme 3	140	135	168.75	443.75	38.07	12.70
	Scheme 4	150	135	168.75	453.75	39.60	12.80
	Scheme 5	160	135	168.75	463.75	40.20	13.43
Change top dressing in turning green-tillering	Scheme 6	141.6	110	168.75	420.35	36.17	12.07
	Scheme 7	141.6	120	168.75	430.35	37.60	12.37
	Scheme 8	141.6	130	168.75	440.35	38.90	12.83
	Scheme 9	141.6	140	168.75	450.35	40.17	13.30
	Scheme 10	141.6	150	168.75	460.35	42.07	14.73
Change top dressing in jointing-heading	Scheme 11	141.6	135	425.6	425.6	35.80	11.77
	Scheme 12	141.6	135	435.6	435.6	37.60	12.37
	Scheme 13	141.6	135	445.6	445.6	39.10	13.17
	Scheme 14	141.6	135	455.6	455.6	41.40	14.90
	Scheme 15	141.6	135	465.6	465.6	43.77	17.50

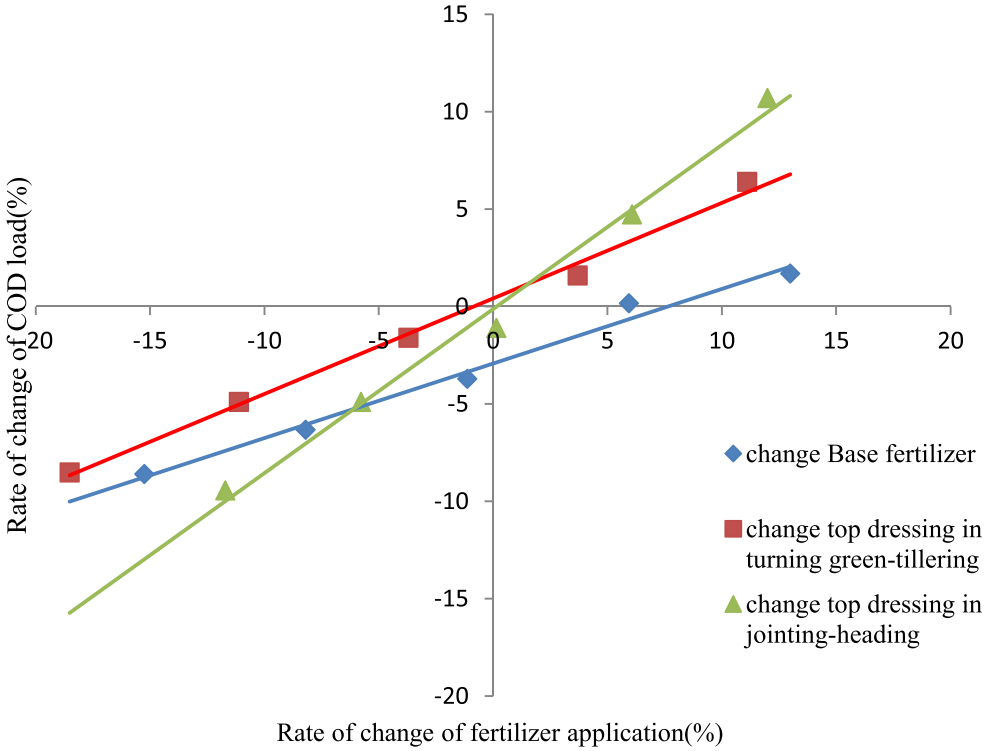

Fig. 5 Sensitive degree of fertilization amount to COD load under different fertilization plan

rate of change of the ammonia nitrogen load is the smallest with the trend line of the change of the basic fertilization amount, and the slope of the second top dressing change is the largest. That is to say, what the three different fertilization schemes are most sensitive to the increase of the field pollution load of ammonia nitrogen is the second top dressing process in jointing-heading, followed by the first top dressing process in turning green-tillering. In comparison, the change of the amount of basic fertilization has little effect on the pollution load of ammonia nitrogen. The impact of field

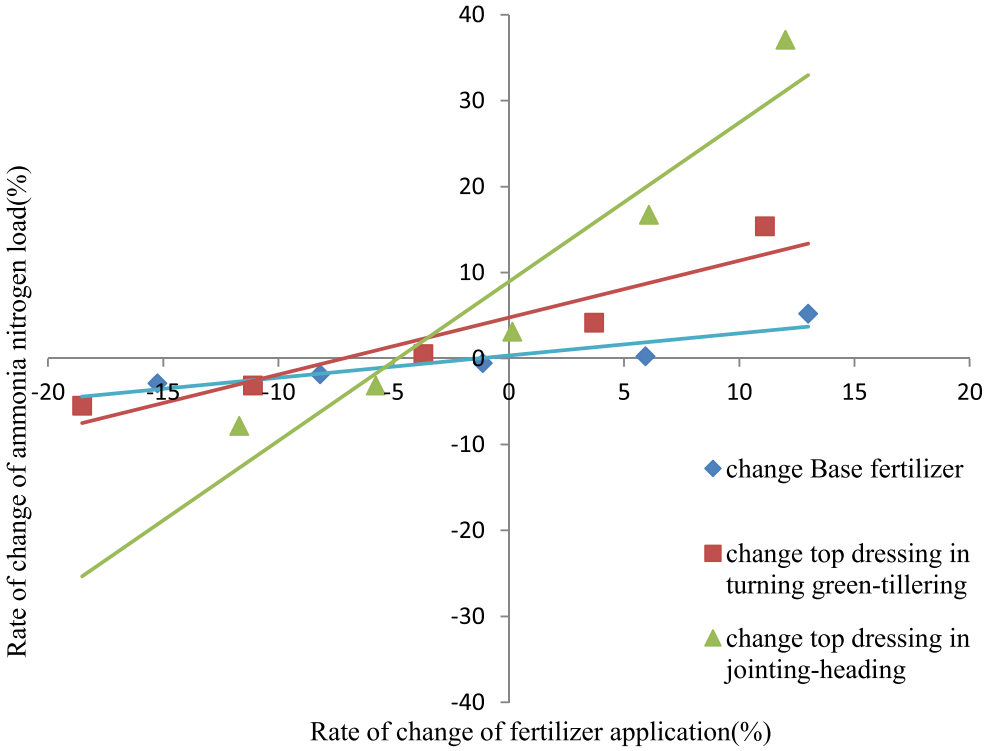

Fig. 6 Sensitive degree of fertilization amount to ammonia nitrogen load intensity under different fertilization plan

pollution load is far greater than that of basic fertilization processes. Based on the above analysis, it can be seen that not only the amount of fertilization applied has an effect on the field pollution load, but even under the same fertilization, the different fertilization schemes also have a greater impact on the field pollution load. Therefore, in the practice of agricultural production, the fertilization schemes should be appropriately adjusted to reduce the non-point source pollution intensity of field agriculture.

The formation mechanism of non-point source pollution in agriculture is complex, and there are many influencing factors, such as crop planting structure, irrigation water amount, fertilization amount and fertilization scheme, and fertilization utilization rate, while the water and fertilization processes are undoubtedly the two main factors determining the intensity of agricultural non-point source pollution in the field. Therefore, rational adjustment and control of the field water and fertilization processes are important measure to prevent non-point source pollution in agriculture.

Conclusions

In this study, one field-scale agricultural non-point pollution model combined evaluation of water discharge and prediction of pollutant concentration in agricultural drain was established in order to estimate the effect of irrigation mount and fertilization on agriculture non-point pollution. Based on the field experiments, the *NSE*, R^2, and *RE* of the COD and ammonia nitrogen load during validation drain are calculated to be above 0.75, 0.81, and less than 15%, respectively, which demonstrated the discriminative power of the established model. Based on the scenario simulation, it is proven that the relationship between the irrigation water amount and field drainage amount is significant and the field pollution load increases with the increase in irrigation amount. Moreover, results show that not only the amount of fertilization applied has an effect on the field pollution load, but even under the same fertilization, the different fertilization schemes also have a greater impact on the field pollution load. It was concluded that the irrigation and fertilization process in field had obvious influence on agricultural non-point source pollution, so taking the control measures to reduce the pollution was important.

Acknowledgments The authors would like to express their sincere gratitude to the anonymous reviewers for their constructive comments and the Editor of the journal. Their detailed suggestions have resulted in an improved manuscript.

Funding information Funding was supported by the National Natural Science Foundation of China (No. 51509223 and No. 51879242).

References

Arnold JG, Srinivasan R, Muttiah RS, Williams JR (1998) Large area hydrologic modeling and assessment part I: model development1. JAWRA J Am Water Resour As 34(1):73–89

Azzellino A, Salvetti R, Vismara R (2006) Combined use of the EPA-QUAL2E simulation model and factor analysis to assess the source apportionment of point and non point loads of nutrients to surface waters. Sci Total Environ 371(1–3):214–222

Bicknell BR, Imhoff JC, Kittle JJL, Jobes THD, JrAS (2011) Hydrological simulation program – Fortran (HSPF): User's manual for release 12. U.S. Environmental Protection Agency, Athens, Ga

Bryan BA (2011) Designing a policy mix and sequence for mitigating agricultural non-point source pollution in a water supply catchment. Water Resour Manag 25(3):875–892

Chen J, Lu J (2014) Establishment of reference conditions for nutrients in an intensive agricultural watershed, eastern China. Environ Sci Pollut R 21(4):2496–2505

Du X, Li X, Zhang W, Wang H (2014) Variations in source apportionments of nutrient load among seasons and hydrological years in a semi-arid watershed: GWLF model results. Environ Sci Pollut R 21(10):6506–6515

Du X, Shrestha NK, Wang J (2019) Integrating organic chemical simulation module into SWAT model with application for PAHs simulation in Athabasca oil sands region, Western Canada. Environ Model Softw 111:432–443

Haas MB, Guse B, Fohrer N (2017) Assessing the impacts of best management practices on nitrate pollution in an agricultural dominated lowland catchment considering environmental protection versus economic development. J Environ Manag 196:347–364

Li X, Weller DE, Jordan TE (2010) Watershed model calibration using multi-objective optimization and multi-site averaging. J Hydrol 380(3):277–288

Li Q, Hu Y, Jia Q et al (2018) Establishment and application of the estimation model for pollutant concentrfation in agriculture drain [C]//IOP conference series: earth and environmental science. IOP Publishing 121(3):032046

Lu H, Xie H (2018) Impact of changes in labor resources and transfers of land use rights on agricultural non-point source pollution in Jiangsu Province, China. J Environ Manag 207:134–140

Moges MA, Schmitter P, Tilahun SA, Steenhuis TS (2018) Watershed modeling for reducing future non-point source sediment and phosphorus load in the Lake Tana Basin, Ethiopia. J Soils Sediments 18(1):309–322

Ongley ED, Xiaolan Z, Tao Y (2010) Current status of agricultural and rural non-point source pollution assessment in China. Environ Pollut 158(5):1159–1168

Pratt B, Chang H (2012) Effects of land cover, topography, and built structure on seasonal water quality at multiple spatial scales. J Hazard Mater 209:48–58

Price K, Purucker ST, Kraemer SR, Babendreier JE, Knightes CD (2014) Comparison of radar and gauge precipitation data in watershed models across varying spatial and temporal scales. Hydrol Process 28(9):3505–3520

Rinaldo A, Benettin P, Harman CJ, Hrachowitz M, McGuire KJ, Velde Y, Bertuzzo E, Botter G (2015) Storage selection functions: a coherent framework for quantifying how catchments store and release water and solutes. Water Resour Res 51(6):4840–4847

Shen Z, Hong Q, Yu H, Liu R (2008) Parameter uncertainty analysis of the non-point source pollution in the Daning River watershed of the three gorges reservoir region, China. Sci Total Environ 405(1):195–205

Shen Z, Chen L, Hong Q, Xie H, Qiu J, Liu R (2013) Vertical variation of nonpoint source pollutants in the three gorges reservoir region. PLoS One 8(8):e71194

Skaggs RW, Youssef MA, Chescheir GM (2012) DRAINMOD: model use, calibration, and validation. T ASABE 55(4): 1509–1522

Wang H, Li X, Hao S (2015a) Effects of rainfall data resolution on watershed-scale model performance in predicting runoff. J Water Clim Chang 6(2):227–240

Wang H, Wu Z, Hu C, Du X (2015b) Water and nonpoint source pollution estimation in the watershed with limited data availability based on hydrological simulation and regression model. Environ Sci Pollut R 22(18):14095–14103

Wang H, Wu Z, Hu C (2015c) A comprehensive study of the effect of input data on hydrology and non-point source pollution modeling. Water Resour Manag 29(5):1505–1521

White RE, Dyson JS, Haigh RA, Jury WA, Sposito G (1986) A transfer function model of solute transport through soil: 2. Illustrative applications. Water Resour Res 22(2):248–254

Woodward SJR, Stenger R, Bidwell VJ (2013) Dynamic analysis of stream flow and water chemistry to infer subsurface water and nitrate fluxes in a lowland dairying catchment. J Hydrol 505:299–311

Wriedt G, Rode M (2006) Modelling nitrate transport and turnover in a lowland catchment system. J Hydrol 328(1–2):157–176

Wu L, Gao JE, Ma XY, Li D (2015) Application of modified export coefficient method on the load estimation of non-point source nitrogen and phosphorus pollution of soil and water loss in semiarid regions. Environ Sci Pollut R 22(14):10647–10660